

# Interaction-induced first order correlation between spatially-separated 1D dipolar fermions

Chi-Ming Chang<sup>(1),(2)</sup>, Wei-Chao Shen<sup>(2)</sup>, Chen-Yen Lai<sup>(2)</sup>, Pochung Chen<sup>(2),(3)</sup> and Daw-Wei Wang<sup>(2),(3)</sup>

<sup>(1)</sup>Physics Department, Harvard University, Cambridge, MA 02138

<sup>(2)</sup>Physics Department, National Tsing-Hua University, Hsinchu, Taiwan 300, ROC

<sup>(3)</sup>Physics Institute, National Center for Theoretical Science, Hsinchu, Taiwan 300, ROC

(Dated: June 2, 2009)

We calculate the ground state properties of fermionic dipolar atoms/molecules in a 1D double-tube potential by using the Luttinger liquid theory and the Density Matrix Renormalization Group calculation. When the external field is applied near a magic angle with respect to the double-tube plane, the long-ranged dipolar interaction can generate a spontaneous correlation between fermions in different tubes, even when the bare inter-tube tunneling rate is negligibly small. Such interaction-induced correlation strongly enhances the contrast of the interference fringes, and therefore can be easily observed in the standard time-of-flight experiment.

## I. INTRODUCTION

Recent progress of ultracold atoms has made it possible to study strongly correlated physics in a much wider parameter range. One of the most important subjects is the one-dimensional (1D) physics, and many interesting phenomena, including Tonks-Girardeau gas [1], Luttinger liquid (LL) behavior [2], and polaronic effects in Bose-Fermi mixture [3], etc. have been theoretically proposed or experimentally observed. However, due to the short-range nature of atomic interaction, it is not easy to study how the interaction between particles in different 1D tubes can bring different many-body effects. In traditional solid state systems, on the other hand, the long-ranged Coulomb interaction between electrons does induce several important many-body features in low dimensional multi-component systems: for example, Coulomb drag between 1D double wires [4], inter-wire/well coherence [5,6], and spontaneous ferromagnetism (or exciton condensation) in double layer quantum Hall systems [7]. Following these extensive studies in the the solid state systems, it is therefore very interesting to investigate how the long-ranged dipolar interaction between ultracold atoms/molecules [8,9] can bring emergent many-body physics in a spatially separated multi-component system, where the first-order and second-order correlation function can be observed easily in a time-of-flight (TOF) measurement. We note that several pioneering works have been reported to explore the exotic quantum phases of bosonic dipolar atoms/molecules [10] in the multi-layer/tube systems, but results for fermionic dipoles seem not well-explored yet to the best of our knowledge.

In this paper, we investigate a 1D double-tube system (see Fig. 1(a), and the similar setup for bosonic atoms in Ref.[11]), where *fermionic* polar molecules [9] (or magnetic dipolar atoms,  $^{53}\text{Cr}$  [8]) are loaded in the ground state of the confinement potential. When no external field is applied, fermions are noninteracting and have no correlation between fermions in the two tubes. Therefore the time-of-flight (TOF) image (imaging light is along the

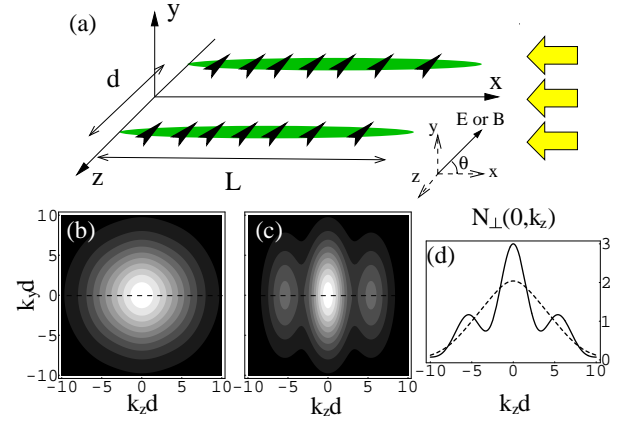


FIG. 1: (Color online) (a) The double-tube system considered in the paper. Tilted arrows indicate the dipole moment of dipolar atoms/molecules. An external field ( $\mathbf{E}$  for the electric field or  $\mathbf{B}$  for the magnetic field) is applied with an angle  $\theta$  in the  $x-y$  plane. The big leftward arrows represent the imaging light for taking a TOF image in the fast expanding (i.e.  $y-z$ ) plane. (b) and (c) are the calculated momentum distribution ( $N_{\perp}(k_y, k_z)$ ), proportional to the TOF image, based on the DMRG result of the lattice model (see Eq. (14) and (15) below). (b) is the noninteracting result, and (c) is the interacting result with  $\theta = \theta_c$ . All the parameters used here are described in the text. The dashed and solid curves in (d) are the amplitude profile along the horizontal line ( $k_y = 0$ ) of (b) and (c) respectively.

tube direction) should be structureless (see Fig. 1(b)). However, when an external electric/magnetic field is applied and tilted near a magic angle,  $\theta_c = \cos^{-1} \sqrt{1/3}$ , the intra-tube dipolar interaction is strongly reduced, leaving only a repulsive and long-ranged *inter-tube* interaction. We show that such exotic interaction can induce the *first-order correlation* between *fermions* in the two tubes, which can be easily measured from the interference fringes (see Fig. 1(c)). We note that unlike the interference between bosons [11,12], the interference between such spatially separated fermionic particles has no counterpart in classical waves, and is induced purely by

the strongly correlated effect.

To investigate this problem systematically, in the following we will first apply the celebrated LL theory with the renormalization group (RG) study in the weakly interacting limit, and then use Density Matrix Renormalization Group (DMRG) method in the strong interaction regime. The weak or strong interaction regime is defined by the ratio between dipolar interaction to the kinetic energy. Results from both calculations assure the existence of such interaction-induced inter-tube correlation, and provide a rich quantum phase diagram. For the convenience of later discussion, we will introduce the pseudo-spin up/down index for the upper/lower tube, so that the conventional definition of magnetic orders can be used to identify the quantum phases in the present system. For example, the ground state with spontaneous inter-tube correlation can be understood as an in-plane ferromagnetic order,  $\langle \hat{\psi}_\uparrow^\dagger(x) \hat{\psi}_\downarrow(x) \rangle \neq 0$ , where  $\hat{\psi}_{\uparrow/\downarrow}(x)$  is the fermionic operator in the upper/lower tube. As a result, the inter-tube correlation can be understood as a 1D planar ferromagnetic (FM) state with the pseudo-spin polarized in the  $x-y$  plane of spin space. This is exactly the 1D version of the well-known spontaneous ferromagnetism in double layer quantum Hall systems [7]. Similar problem about 1D ferromagnetism of itinerant fermions is also an important subject discussed in the literature [13]. Note that the pseudo-spin defined here has nothing to do with the original spin of fermionic dipoles.

## II. HAMILTONIAN AND LUTTINGER LIQUID THEORY IN THE WEAKLY INTERACTING LIMIT

Throughout this paper, we will assume that particles are loaded in the lowest subband of each tube with a transverse confinement wavefunction  $\phi_s(y, z) = \frac{1}{\sqrt{\pi}R} e^{-(y^2+(z-sd)^2)/2R^2}$  and a Gaussian radius  $R$  (here  $s = \pm \frac{1}{2} = \uparrow / \downarrow$  is the pseudo-spin index). The resulting effective 1D system Hamiltonian then can be written to be  $H = H_0 + H_I$ , where  $H_0$  is the kinetic energy:

$$H_0 = \sum_s \int_0^L dx \hat{\psi}_s^\dagger(x) \frac{-\hbar^2}{2m} \partial_x^2 \hat{\psi}_s(x) \quad (1)$$

with  $m$  being the mass of dipolar particles, and  $H_I$  is the interaction energy:

$$H_I = \frac{1}{2} \sum_{s,s'} \int_0^L dx \int_0^L dx' V_{|s-s'|}(x-x') \times \hat{\psi}_s^\dagger(x) \hat{\psi}_s(x) \hat{\psi}_{s'}^\dagger(x') \hat{\psi}_{s'}(x'). \quad (2)$$

Here  $V_{|s-s'|}(x)$  is the dipolar interaction between molecules in the same tubes ( $V_0$ ) and/or in different tubes ( $V_1$ ), obtained by integrating out the transverse degree of freedom:  $V_{|s-s'|}(x) \equiv \int d\mathbf{r}_{1,\perp} \int d\mathbf{r}_{2,\perp} |\phi_s(\mathbf{r}_{1,\perp})|^2 |\phi_{s'}(\mathbf{r}_{2,\perp})|^2 V_d(\mathbf{r}_1 - \mathbf{r}_2)$ ,

where  $V_d(\mathbf{r}) = D^2(1 - 3(\hat{r} \cdot \hat{E})^2)/|\mathbf{r}|^3$  is the bare dipolar interaction with  $D$  being the electric dipole moment in c.g.s unit.  $\hat{E}$  is the unit vector along the external electric field. Since in general the electric dipole interaction is much stronger (and tunable) than the magnetic dipole interaction, in the the rest of this paper we will use polar molecules as the underlying particles for further discussion. Extension to the magnetic dipolar atoms is straightforward.

Defining  $\tilde{V}_{0/1}(k) \equiv \int dx V_{0/1}(x) e^{-ikx}$  to be the Fourier transform of interaction, we can calculate their zero momentum ( $k = 0$ ) value analytically by integrating over the transverse confinement wavefunction,  $\phi_s(\mathbf{r}_\perp)$ :

$$\tilde{V}_0(0) = \frac{D^2(1 - 3\cos^2\theta)}{R^2} \quad (3)$$

$$\tilde{V}_1(0) = D^2 \left( 2 - \left( 2 + \frac{d^2}{R^2} \right) e^{-\frac{d^2}{2R^2}} \right) \frac{\sin^2\theta}{d^2}. \quad (4)$$

It is very easy to see that when  $\theta \sim \theta_c = \cos^{-1} \sqrt{1/3}$  the intra-tube interaction is almost zero while the inter-tube interaction is still finite and positive. Such interesting kind of interaction matrix element cannot be realized in the traditional solid state system and therefore may bring some physics not predicted before.

In the weakly interacting limit, we can apply the standard LL theory [14] by linearizing the band energy around the two Fermi points,  $\pm k_F$ , and dividing fermions into the left/right movers (i.e.  $\hat{\psi}_s(x) = \sum_{r=\pm} \hat{\psi}_{r,s}(x)$ , where  $r = \pm$  is the chiral index). The resulting low energy effective Hamiltonian can be rewritten to be,  $H_{\text{eff}} = H_{\text{LL}} + H_1$ , where

$$H_{\text{LL}} = v_F \int_0^L dx \sum_{r,s} \hat{\psi}_{r,s}^\dagger(x) \left( -i\hbar \frac{\partial}{\partial x} - k_F \right) \hat{\psi}_{r,s}(x) + \frac{1}{2} \sum_{r,r',s,s'} \tilde{g}_{s,s'}^{r,r'} \int_0^L dx \hat{\rho}_{r,s}(x) \hat{\rho}_{r',s'}(x) \quad (5)$$

is the LL Hamiltonian with the density operator,  $\hat{\rho}_{r,s}(x) \equiv \hat{\psi}_{r,s}^\dagger(x) \hat{\psi}_{r,s}(x)$  and the forward scattering amplitude:  $\tilde{g}_{s,s'}^{r,r'} \equiv \tilde{V}_{|s-s'|}(0) - g_{\parallel} \delta_{r,-r'} \delta_{s,s'}$ ;

$$H_1 \equiv g_{\perp} \sum_s \int_0^L dx \hat{\psi}_{+,s}^\dagger(x) \hat{\psi}_{-,s}(x) \hat{\psi}_{-,s}^\dagger(x) \hat{\psi}_{+,s}(x) \quad (6)$$

is the backward scattering between particles of different tubes and different chiralities. Here  $v_F$  is the Fermi velocity, and  $g_{\parallel/\perp} \equiv \tilde{V}_{0/1}(2k_F)$  is the backward scattering amplitude. According to the standard Luttinger theory [14], the linearized band structure about the two Fermi points is justified only when the interaction strength is much smaller than the Fermi energy, i.e. when

$$\frac{D^2}{R^3} \ll \frac{\hbar^2 k_F^2}{2m}. \quad (7)$$

It is well-known that the LL Hamiltonian,  $H_{\text{LL}}$ , can be diagonalized exactly via a Bogoliubov transformation,

while the backward scattering term,  $H_1$ , cannot be diagonalized in the same basis. As a result, we have to use the standard one-loop renormalization group (RG) calculation [14] to investigate when the later term is relevant in the low energy limit, and how it renormalizes the former one ( $H_{LL}$ ) in different parameter regime. The bare Luttinger exponents are given by the initial system parameters,

$$K_{\rho/\sigma} \equiv \sqrt{\frac{\pi v_F + \frac{1}{2}g_{\parallel}}{\pi v_F + \tilde{V}_{\rho/\sigma} - \frac{1}{2}g_{\parallel}}}, \quad (8)$$

where  $\tilde{V}_{\rho/\sigma} \equiv \tilde{V}_0(0) \pm \tilde{V}_1(0)$ . Within the one-loop RG, only  $K_{\sigma}$  and the backward scattering,  $g_{\perp}$ , are renormalized [14], following the RG equations below:

$$\frac{dK_{\sigma}}{dl} = -\frac{1}{2}K_{\sigma}^2 \left( \frac{g_{\perp}}{\pi v_{\sigma}} \right)^2, \quad \frac{dg_{\perp}}{dl} = 2g_{\perp}(1 - K_{\sigma}), \quad (9)$$

where

$$v_{\sigma} \equiv \sqrt{(v_F + \tilde{V}_{\sigma}/\pi)^2 - (\tilde{V}_{\sigma}/\pi)^2} \quad (10)$$

is the collective mode velocity of the (pseudo-)spin-mode sector.  $l = \ln \Lambda$  is the scaling parameter with  $\Lambda$  being the shortest length scale (or the largest momentum scale) in the present system. For a given bare system parameter,  $(K_{\sigma}, g_{\perp})$ , Eq. (9) then shows how they can flow to a fixed point,  $(K_{\sigma}^*, g_{\perp}^*)$ , which determines the true low energy physical properties of the double-tube system.

### III. PHASE DIAGRAM IN THE LUTTINGER LIQUID THEORY

To obtain a quantum phase diagram in the LL theory, we have to use the RG result to calculate the scaling exponent,  $\alpha$ , of various correlation function in the long-distance limit, i.e.  $\langle \hat{O}^{\dagger}(x)\hat{O}(0) \rangle \sim x^{-2+\alpha}$  as  $|x| \rightarrow \infty$ , where  $\hat{O}(x)$  is the order parameter operator of interest. For a given system parameter, the dominant order parameter is then determined by the most slowly decaying correlation function (or the largest and positive  $\alpha$ ), known as the quasi-long-ranged order in 1D systems. Similar to the standard Luttinger liquid theory for other 1D systems [14], we investigate the following candidates of order parameters [14], because scaling exponents for other more complicated kinds of order parameters are always smaller than the ones below and therefore becomes negligible. The definitions of order parameters we considered in this paper includes (the associated scaling exponent is shown after the definition): Wigner crystal ( $\hat{O}_{WC} = \sum_s \hat{\psi}_{+,s}^{\dagger} \hat{\psi}_{+,s}^{\dagger} \hat{\psi}_{-,s}^{\dagger} \hat{\psi}_{-,s}$ ,  $\alpha_{WC} = 2 - 4K_{\rho}$ ), charge density wave ( $\hat{O}_{CDW} = \sum_s \hat{\psi}_{+,s}^{\dagger} \hat{\psi}_{-,s}$ ,  $\alpha_{CDW} = 2 - K_{\rho} - K_{\sigma}$ ), axial (pseudo-)spin density wave ( $\hat{O}_{SDW_z} \equiv \sum_{s,s'} \hat{\sigma}_{s,s'}^z \hat{\psi}_{+,s}^{\dagger} \hat{\psi}_{-,s'}$ ,  $\alpha_{SDW_z} = 2 - K_{\rho} - K_{\sigma}$ ), planar (pseudo-)spin density wave ( $\hat{O}_{SDW_{x,y}} \equiv$

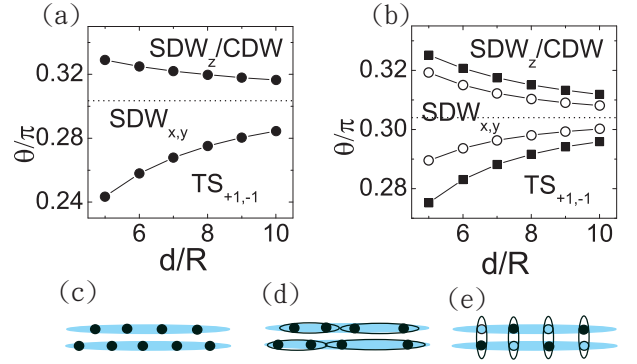


FIG. 2: (Color online) Quantum phase diagrams in terms of the tube separation relative to the tube radius,  $d/R$ , and the tilted angle,  $\theta/\pi$ , in the LL theory. (a)  $k_F R = 0.1$  (filled circle), (b)  $k_F R = 0.2$  (filled square) and  $k_F R = 0.4$  (open circle). The dashed line indicates the magic angle,  $\theta_c = \cos^{-1} \sqrt{1/3} \approx 0.304\pi$ . (c)-(e) are cartoons to represent the axial SDW, polarized triplet superfluid, and the planar SDW phases respectively as defined in the text (also consistent with the literature [14]). The filled and open circles here indicate the particle and hole fluctuation respectively. The horizontal ellipses in (d) indicate pairing between fermionic particles, while the vertical ellipses in (e) indicates an inter-tube correlation (i.e. there is an uncertainty for the particle position between the two tubes). The average particle density distribution is uniform for  $SDW_{x,y}$  phase (e), while it is staggered for  $SDW_z$  phase (c), which has no inter-tube correlation.

$\sum_{s,s'} \hat{\sigma}_{s,s'}^{x,y} \hat{\psi}_{+,s}^{\dagger} \hat{\psi}_{-,s'}$ ,  $\alpha_{SDW_{x,y}} = 2 - K_{\rho} - K_{\sigma}^{-1}$ , and here  $\hat{\sigma}_{ij}^{x,y,z}$  is Pauli matrix element), singlet superfluid ( $\hat{O}_{SS} \equiv \sum_s s \hat{\psi}_{+,s} \hat{\psi}_{-,s}$ ,  $\alpha_{SS} = 2 - K_{\rho}^{-1} - K_{\sigma}$ ), unpolarized triplet superfluid ( $\hat{O}_{TS_0} \equiv \sum_s \hat{\psi}_{+,s} \hat{\psi}_{-,s}$ ,  $\alpha_{TS_0} = 2 - K_{\rho}^{-1} - K_{\sigma}$ ), and polarized triplet superfluid ( $\hat{O}_{TS_{2s}} \equiv \hat{\psi}_{+,s} \hat{\psi}_{-,s}$  for  $s = \pm 1/2$ ,  $\alpha_{TS_{2s}} = 2 - K_{\rho}^{-1} - K_{\sigma}^{-1}$ ). In the low energy limit, the exponent  $\alpha$  for each phase is then obtained from the renormalized Luttinger exponents,  $K_{\sigma}^*$  (obtained via solving Eq. (9)) and  $K_{\rho}^* = K_{\rho}$ . Note that  $K_{\rho}^*$  is not renormalized within the one-loop RG scheme and therefore is the same as the initial(bare) value obtained from the system parameters.

After calculating the scaling exponents of various order parameters mentioned above, we find that only three of them can be the dominant phases in the system we consider here. They are axial (pseudo-)spin density wave ( $SDW_z$ ), planar (pseudo-)spin density wave ( $SDW_{x,y}$ ), and polarized triplet superfluid ( $TS_{\pm}$ ). The charge density wave (CDW) has the same scaling exponent as  $SDW_z$ , but it can be shown that it still decay fast than the later case by a logarithmic correction after integrating along the RG flow [14]. In this paper, we will still consider both of them to be the dominant phase, but only discuss the physics related to the  $SDW_z$  order for simplicity. From the definition of scaling exponent above, it is easy to see that the phase boundary between the planar (pseudo-)spin density wave ( $SDW_{x,y}$ ), and the polarized

triplet superfluid ( $TS_{\pm}$ ) is determined by  $K_{\rho}^* = K_{\rho} = 1$ , while the phase boundary between the axial (pseudo-)spin density wave ( $SDW_z$ ) and the planar (pseudo-)spin density wave ( $SDW_{x,y}$ ) is by  $K_{\sigma}^* = 1$ . From the expression of the bare LL exponent in Eq. (8), we can find the first phase boundary is then determined by the following simple equation:

$$\tilde{V}_{\rho} = \tilde{V}_0 + \tilde{V}_1 = g_{\parallel} = \tilde{V}_0(2k_F). \quad (11)$$

However, when considering the phase boundary between  $SDW_z$  and  $SDW_{x,y}$ , we have to calculate the renormalized Luttinger exponent,  $K_{\sigma}^*$ , from the RG equation in Eq. (9). Integrating Eq. (9) directly, it is easy to show that the solution connecting to  $K_{\sigma}^* = 1$  and  $g_{\perp}^* = 0$  (required as a fixed point of Eq. (9),  $dK_{\sigma}/dl = dg_{\perp}/dl = 0$ ) is given by

$$1 - \frac{1}{K_{\sigma}} - \ln K_{\sigma} = -\frac{1}{8} \left( \frac{g_{\perp}}{\pi v_{\sigma}} \right)^2. \quad (12)$$

To obtain the functional dependence of the interaction strength on this RG line, we can insert the bare form of  $K_{\sigma}$  in Eq. (8) and take the weak interaction limit. The leading order terms then give the following condition for the phase boundary between  $SDW_z$  and  $SDW_{x,y}$ :

$$\begin{aligned} \tilde{V}_{\sigma} &= \tilde{V}_0 - \tilde{V}_1 \\ &= g_{\perp} + g_{\parallel} = \tilde{V}_0(2k_F) + \tilde{V}_1(2k_F). \end{aligned} \quad (13)$$

Since each term in Eqs. (11) and (13) is proportional to  $D^2$ , the phase boundary lines determined above are independent of the interaction strength (more precisely, true only in the weak interaction limit). As a result, the phase diagram of LL theory can be completely determined by the following three dimensionless parameters:  $d/R$ ,  $\theta$ , and  $k_F R$ .

In Figs. 2(a) and (b), we show the calculated phase diagram as a function of  $d/R$  and  $\theta$ , for three different values of particle density,  $k_F R$ . For a given inter-tube separation,  $d$ , the system is dominated by the axial (pseudo-)spin density wave ( $SDW_z$ ) in the regime of large tilted angle  $\theta$ . Such state can be also understood as a “phase-locked” state with staggered modulation of the particle density (see Fig. 2(c)), similar to the 1D electron gas in the semi-conductor double wire system [15]. This phase results from the fact that when  $\theta$  is large, the intra-tube interaction is repulsive and stronger than the inter-tube interaction, making a crystalized density distribution in each tube. At the same time, the backward scattering,  $g_{\perp}$ , scales to be infinite (i.e.  $g_{\perp}^* \rightarrow \infty$  because  $K_{\sigma}^* < 1$ , see Eq. (9)), and therefore opens a single particle excitation gap. Such divergence of  $g_{\perp}$  also leads to a vanishing  $K_{\sigma}^*$  according to Eq. (9). This is why the scaling exponent of  $SDW_z$  becomes much larger than  $SDW_{x,y}$  in the low energy limit (see above for the definition of scaling exponents for each phase). In the regime of small  $\theta$ , on the other hand, the intra-tube interaction becomes attractive, leading to a triplet superfluid ( $TS_{\pm}$ )

(Fig. 2(d)). It is easy to see from the order parameters of the above two phases, there is no inter-tube correlation, and therefore no visible interference fringes in the fast expanding plane, similar to the noninteracting result in Fig. 1(b).

However, when  $\theta$  is in the intermediate range and close to  $\theta_c \sim 0.304\pi$ , the ground state becomes the planar (pseudo-)spin density wave ( $SDW_{x,y}$ ). In this parameter regime, the intra-tube interaction becomes smaller than the inter-tube interaction (i.e.  $|\tilde{V}_0(0)| < \tilde{V}_1(0)$ , see Eqs. (3)-(4)), and therefore the backward scattering becomes *irrelevant* in the low energy limit ( $g_{\perp}^* \rightarrow 0$  because  $K_{\sigma}^* > 1$ , see Eq. (9)), leading to a *uniform* density distribution along the tube. Besides, the order parameter,  $\hat{O}_{SDW_{x,y}}$ , has implied that at each position on the tube, fermionic particles has equal and non-zero probability to be found in the upper and the lower tube (or say, there is an uncertainty for a particle to be in one tube or the other, although the average probability in these two tubes are the same), showing an interaction induced inter-tube correlation (with a periodic modulation of the relative gauge phase, see Fig. 2(e)). Although within the LL theory, such inter-tube correlation is a quasi-long-ranged order, we still expect to observe it in the interference pattern (similar to Fig. 1(c)) in a finite size system after integrating along the tube direction, if only the scaling exponent,  $\alpha$ , is not too small. For typical parameters of polar molecules, say OH molecules ( $m \sim 17$  a.m.u. and the largest dipole moment is  $D \sim 1.68$  Debye), we can consider  $R \sim 0.1 \mu\text{m}$ ,  $d \sim 0.5 \mu\text{m}$ , and  $k_F \sim \pi \times 10 \mu\text{m}^{-1}$ , and hence the obtained  $\alpha_{SDW_{x,y}}$  can be of the order of 0.1 or more, showing that the probability to observe such inter-tube correlation is not small. We note that this planar (pseudo-)SDW $_{x,y}$  phase with a spontaneous inter-tube correlation is a completely new phase, and has no counterpart even in the traditional solid state (semi-conductor or metal) double-wire system.

#### IV. FERROMAGNETISM IN STRONGLY INTERACTING REGIME

In the strongly interacting regime (i.e. the interaction energy is of the same order of or even larger than Fermi energy), LL theory fails to give correct low energy physics and hence we apply DMRG method to numerically study the ground state properties. For the convenience of numerical calculation, from now on we will consider  $\theta = \theta_c$  only to eliminate the intra-tube interaction completely. Besides, we assume an optical lattice is applied along the tube direction ( $x$ ) so that the system Hamiltonian can be written in a single band lattice model:

$$\begin{aligned} H_{\text{lat}} &= -t \sum_{j,s} \left( \hat{a}_{j,s}^{\dagger} \hat{a}_{j+1,s} + h.c. \right) - J \sum_{j,s} \hat{a}_{j,s}^{\dagger} \hat{a}_{j,-s} \\ &+ U \sum_j \hat{n}_{j,\uparrow} \hat{n}_{j,\downarrow} + \frac{V}{2} \sum_{\langle j_1, j_2 \rangle, s} \hat{n}_{j_1, s} \hat{n}_{j_2, -s} \end{aligned} \quad (14)$$

where  $\hat{a}_{j,s}$  and  $\hat{n}_{j,s} = \hat{a}_{j,s}^\dagger \hat{a}_{j,s}$  here are the fermionic field operator and density operator of the site  $j$  and the pseudo-spin  $s = \uparrow / \downarrow$ . Here  $t$ ,  $J$ ,  $U$ , and  $V$  are the inter-site tunneling in the same tube, the inter-tube tunneling, the inter-tube onsite repulsion, and the inter-tube nearest-neighboring-site repulsion respectively. Note that we introduce inter-tube tunneling  $J$  here just for the completeness of numerical calculation, but we will just concentrate on the physics in the limit of zero  $J$  after the calculation, i.e. in the limit of zero inter-tube tunneling. The numerical values of these parameters can be easily calculated by integrating over the on-site Wannier function, and can be tuned in a wide range by changing the external field strength, lattice strength, and/or lattice spacing. Since it is not our purpose in this paper to provide a numerical comparison with any certain experimental setup (there is unfortunately no such system available yet), we will not calculate their absolute values in this paper, but will present all of our results in dimensionless parameters instead. For simplicity, we also have neglected the interaction of longer (next-nearest-neighboring sites) range.

In Fig. 3 we first show the ground state energy,  $E_G$ , as a function of  $V$ , by taking  $J = 0$ ,  $U/t = 3$  and the total particles,  $N = 10$ , in a 1D lattice of length  $L = 20$ . Note that by taking  $J = 0$ , particle numbers in each tube is a conserved quantity and therefore we can label the system eigenstates by  $(N_\uparrow, N_\downarrow)$ . There are three different regimes of interest: in regime I ( $V < 1.317$ ),  $E_G$  increases linearly as a function of  $V$ , and the numbers of particles in the two tubes are the same ( $N_\uparrow = N_\downarrow = 5$ ) in the ground state. Detailed analysis shows that the ground state wavefunction is the same as the SDW<sub>*x,y*</sub> phase in the weak interaction limit discussed above. In regime III ( $V > 1.321$ ),  $E_G$  becomes independent of  $V$ , because all particles are moved to either one of the tubes to minimize the strong inter-tube interaction energy. This phase can be described as an axial ferromagnetic state by breaking the  $Z_2$  (spatial inversion) symmetry of the Hamiltonian, Eq. (14). Inside the narrow window of regime II ( $1.317 < V < 1.321$ ), the ground state energy changes step by step as the particle number difference changes, indicating a series of first order phase transitions. In the thermodynamic limit ( $N, L \gg 1$ ), it is reasonable to expect that the ground state energy should become a smooth curve in regime II, i.e. an *infinitesimal* inter-tube tunneling ( $J \rightarrow 0$ ) can easily mix many degenerate states and lead to a coherent ground state,  $|\Psi_C\rangle$ , which has finite single particle inter-tube correlation between fermions in the two spatially separated tubes. Using the language of magnetism, we can define the pseudo-spin magnetization density to be  $\vec{\mathcal{M}} \equiv \frac{1}{N} \sum_j \sum_{s,s'} \vec{\sigma}_{s,s'} \hat{a}_{j,s}^\dagger \hat{a}_{j,s'}$ , and such spontaneous inter-tube correlation can be understood as an in-plane ferro-magnetization, i.e.  $\langle \Psi_C | \mathcal{M}_x | \Psi_C \rangle \neq 0$ .

To confirm this conjecture, we further investigate results with a finite but small inter-tube tunneling,  $J$ , which is equivalent to an effective "magnetic field" along

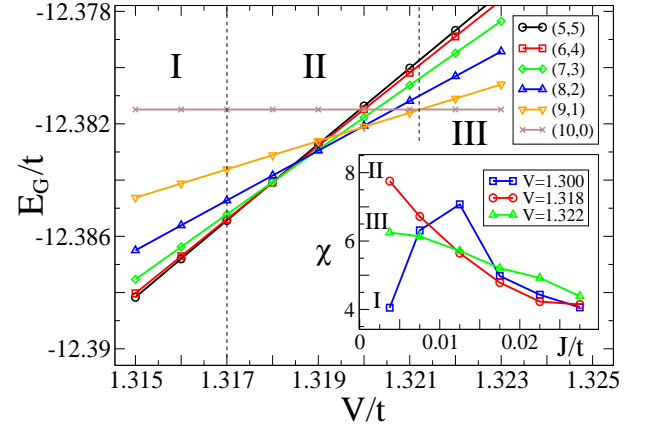


FIG. 3: (Color online) Ground state energy of Eq. (14) (for  $J = 0$ ) as a function of  $V/t$  for different particle numbers in the two tubes,  $(N_\uparrow, N_\downarrow)$ . Regime I, II, and III are the SDW<sub>*x,y*</sub>, canted ferromagnetic (or inter-tube correlated) phase, and axial ferromagnetic phase respectively. The detailed definition is in the text. Inset shows the magnetic susceptibility  $\chi$  (defined in the text) as a function of inter-tube hopping,  $J$ .

the  $x$  direction in the *pseudo-spin space*. In other words, we can study how the system magnetization responds to such small perturbation by calculating the "magnetic" susceptibility,  $\chi \equiv \partial \langle \Psi_C | \mathcal{M}_x | \Psi_C \rangle / \partial J$ . As shown in the inset of Fig. 3,  $\chi$  has a tendency to diverge as  $J \rightarrow 0$  when  $V$  is tuned to be inside the regime II, strongly indicating an in-plane FM order. Combining the fact that the average numbers of particles in the two tubes are also different in this regime (i.e.  $\langle \Psi_C | \mathcal{M}_z | \Psi_C \rangle \neq 0$ , as indicated from Fig. 3), the ground state in regime II is best understood as a pseudo-spin canted ferromagnetism, i.e. pseudo-spin is uniformly polarized with a tilted angle about the pseudo-spin  $z$  axis. This is another striking new phase predicted in this paper, breaking a continuous  $U(1)$  symmetry in 1D system. Different from the planar SDW discussed in the weakly interacting limit, the pseudo-spin FM state obtained here in the strongly interacting regime has a uniform (rather than periodic oscillation) magnetization. From the experimental point of view, this order parameter indicates a strong interference fringes as shown in Fig. 1(c). Unfortunately, so far we have not been able to calculate systems of larger size with an efficient code, and therefore the demonstration of the existence of such symmetry breaking state in the thermodynamic limit may need more justification. However, to the best of our knowledge, our system is probably the first *physical* candidate (rather than a mathematical model) to realize the ferromagnetism of 1D itinerant fermions: it is not restricted by the celebrated Lieb-Mattis theorem [16] or Mermin-Wigner theorem [17] due to the nontrivial long-ranged and anisotropic dipolar interaction. Numerical results for larger system size and more complete phase diagram of this double-tube system should be an interesting direction to explore in the future.

## V. INTERFERENCE PATTERN IN THE TIME-OF-FLIGHT EXPERIMENT

Since the theme of this paper is to demonstrate the existence of an interaction-induced inter-tube correlation between 1D dipolar fermions (true for both weak and strong interaction regime), the best experimental evidence is from the interference pattern between these fermions. Theoretically, we can calculate the momentum distribution function of the ground state and then integrate along the tube direction to obtain the TOF image in the fast expanding ( $y - z$ ) plane,  $N_{\perp}(\mathbf{k}_{\perp})$  (here  $\mathbf{k}_{\perp} \equiv (k_y, k_z)$ , see Fig. 1). Since particles can fly fast from the tube center after the strong confinement potential is released, such TOF image should eventually become equivalent to momentum distribution after a long time of flight. After integrating out the contribution along the tube direction ( $x$ ), we can obtain the following expression for  $N_{\perp}(\mathbf{k}_{\perp})$ :

$$N_{\perp}(\mathbf{k}_{\perp}) = 4\pi R^2 N e^{-|\mathbf{k}_{\perp}|^2 R^2} (1 + 2\langle \mathcal{M}_x \rangle \cos(k_z d)) \quad (15)$$

where we have used a Gaussian type-wavefunction (with radius  $R$ ) to approximate the initial confinement wavefunction,  $\phi_s(\mathbf{r}_{\perp})$ , and  $\langle \mathcal{M}_x \rangle \equiv \langle \Psi_C | \mathcal{M}_x | \Psi_C \rangle$  is the inter-tube correlation. When the inter-tube tunneling,  $J$ , is small and the interaction is weak, the calculated inter-tube correlation ( $\langle \mathcal{M}_x \rangle$ ) is so small that the obtained momentum distribution (i.e. TOF image) is close to a broad Gaussian-like function without any structure (see Fig. 1(b) and the dashed line in Fig. 1(d)). On the other hand, when the direction and the strength of dipolar interaction is tuned to the regime II of Fig. 3, the long-ranged inter-tube interaction strongly enhances the inter-tube correlation ( $\langle \mathcal{M}_x \rangle$ ) and hence the contrast of interference fringes. In Fig. 1(c) (and the solid line in Fig. 1(d)), we show a typical calculated interference pattern (i.e.  $N_{\perp}(\mathbf{k})$ ) with parameters in this regime:  $U/t = 3$ ,  $V/t = 1.318$ , and  $R/d = 0.167$  for quarter-filling ( $L = 20$  and  $N = 10$ ). We find that even the same single particle inter-tube tunneling rate ( $J/t = 0.1$ ) is used in the calculation of both Fig. 1(b) and (c), the obtained interference patterns are totally different: the later has strong contrast in the interference fringes due to the interaction effect. Unlike the usual interference fringes between bosonic particles, the fermionic dipoles here do not have a condensate in each tube, and therefore has no counterpart in any classical waves.

As for the quasi-long-ranged order predicted by the Luttinger liquid theory in the weakly interacting regime, one should measure the TOF image in the  $x - z$  plane by using the imaging light perpendicular to the double tube plane ( $y$ ). As a result both  $\text{SDW}_z$  and  $\text{SDW}_{x,y}$  phases can show some kinds of Bragg peaks along the  $x$ -axis due to the periodic distribution of density and/or phase fluctuations, while the  $\text{TS}_{\pm 1}$  phase does not have such feature. Furthermore,  $\text{SDW}_z$  phase has a single particle gap, while  $\text{SDW}_{x,y}$  and  $\text{TS}_{\pm 1}$  do not have such gap. This gap can be easily measured by light scattering spectroscopy and hence becomes a way to distinguish these two density wave phases. We note that although the inter-tube correlation of  $\text{SDW}_{x,y}$  phase is periodically oscillating and the correlation function decays as a power-law in large distance, the finite tube length can still make it possible to measure some residual inter-tube correlation, which does not exist in the other two phases. According to the results of bosonic atoms [11,18], the noise correlation of the TOF image for different lengths of tube can also provide the experimental value of the Luttinger exponent.

## VI. SUMMARY

In this paper, we find an interaction-induced inter-tube correlation between spatially-separated fermionic polar molecules (or dipolar atoms) in the 1D double-tube potential. Such correlation does not exist if the interaction between fermions is too weak, showing a clearly many-body effect in a 1D system. We use both Luttinger liquid theory (with proper renormalization group method) to study the phase diagram in weak interaction limit, and use Density Matrix Renormalization Group Method to calculate the order parameters in strong interaction regime. This new phenomenon predicted in this paper can be observed in the first order interference pattern, and has no counterpart either in the classical waves or in the 1D solid state systems.

## VII. ACKNOWLEDGEMENT

We thank S. Das Sarma, G. Fiete, I. Spielman, and H.-H. Lin for fruitful discussions. This work is supported by NSC via NCTS in Taiwan.

<sup>1</sup> B. Paredes, A. Widera, V. Murg, O. Mandel, S. Fölling, I. Cirac, G. V. Shlyapnikov, T. W. Hänsch and I. Bloch, *Nature* **429**, 277 (2004); T. Kinoshita, T. Wenger, and D. S. Weiss, *Science* **305**, 1125 (2004).

<sup>2</sup> For a recent review of Luttinger liquid theory in 1D Bose gas, see M. A. Cazalilla, *J. Phys. B: AMOP* **37**, S1 (2004); M. A. Cazalilla, A. F. Ho, and T. Giamarchi, *New J. Phys.*

**8**, 158 (2006).

<sup>3</sup> L. Mathey, D.-W. Wang, W. Hofstetter, M. D. Lukin, and E. Demler, *Phys. Rev. Lett.* **93**, 120404 (2004); L. Mathey and D.-W. Wang, *Phys. Rev. A* **75**, 013612 (2007).

<sup>4</sup> P. Debray, V. Zverev, O. Raichev, R. Klesse, P. Vasilopoulos and R. S. Newrock, *J. Phys. Condens. Matter* **13**, 3389 (2001); P. Debray, V. N. Zverev, V. Gurevich, R.



- Klesse and R. S. Newrock, *Semicond. Sci. Technol.* **17**, R21 (2002); M. Yamamoto, M. Stopa, Y. Tokura, Y. Hirayama, S. Tarucha, *Physica* **12E** 726 (2002).
- <sup>5</sup> D.-W. Wang, E. G. Mishchenko, and E. Demler, *Phys. Rev. Lett.* **95**, 086802 (2005).
- <sup>6</sup> L. Zheng, M. W. Ortalano, and S. Das Sarma, *Phys. Rev. B* **55**, 4506 (1997);
- <sup>7</sup> I. B. Spielman, J. P. Eisenstein, L. N. Pfeiffer, and K. W. West, *Phys. Rev. Lett.* **87**, 036803 (2001); M. Kellogg, J. P. Eisenstein, L. N. Pfeiffer, and K. W. West, *Phys. Rev. Lett.* **90**, 246801 (2003); M. Kellogg, J. P. Eisenstein, L. N. Pfeiffer, and K. W. West, *Phys. Rev. Lett.* **93**, 036801 (2003). For a review of bilayer QH effect, see S. M. Girvin and A. H. MacDonald, in *Perspectives in Quantum Hall Effects* edited by S. Das Sarma and A. Pinczuk (John Wiley & Sons, New York, 1997); J. P. Eisenstein, *ibid*, and reference therein.
- <sup>8</sup> J. Stuhler<sup>1</sup>, A. Griesmaier, T. Koch<sup>1</sup>, M. Fattori, T. Pfau, S. Giovanazzi, P. Pedri, and L. Santos, *Phys. Rev. Lett.* **95**, 150406 (2005); T. Lahaye, T. Koch, B. Fröhlich, M. Fattori, J. Metz, A. Griesmaier, S. Giovanazzi, and T. Pfau, *Nature* **448**, 672 (2007); T. Koch, T. Lahaye, J. Metz, B. Fröhlich, A. Griesmaier, and T. Pfau, *Nature Physics* **4**, 218 (2008).
- <sup>9</sup> K.-K. Ni, S. Ospelkaus, M. H. G. de Miranda, A. Pe'er, B. Neyenhuis, J. J. Zirbel, S. Kotochigova, P. S. Julienne, D. S. Jin, and J. Ye, *Science* **322**, 231 (2008).
- <sup>10</sup> D.-W. Wang, M. D. Lukin, and E. Demler, *Phys. Rev. Lett.* **97**, 180413 (2006); D.-W. Wang, *Phys. Rev. Lett.* **98**, 060403 (2007); A. Arguelles and L. Santos, *Phys. Rev. A* **75**, 053613 (2007); C. Kollath, Julia S. Meyer, and T. Giamarchi<sup>1</sup>, *Phys. Rev. Lett.* **100**, 130403 (2008).
- <sup>11</sup> A. Polkovnikov, E. Altman, and E. Demler, *PNAS* **103**, 6125 (2006); V. Gritsev, E. Altman, E. Demler and A. Polkovnikov, *Nature Phys.* **2**, 705 (2006); S. Hofferberth, I. Lesanovsky, T. Schumm, A. Imambekov, V. Gritsev, E. Demler, and J. Schmiedmayer, *Nature Phys.* **4**, 489 (2008).
- <sup>12</sup> M. R. Andrews, C. G. Townsend, H.-J. Miesner, D. S. Durfee, D. M. Kurn, and W. Ketterle, *Science* **275**, 637 (1997).
- <sup>13</sup> E. Lieb, *Phys. Rev. Lett.* **62**, 1201 (1989); A. Mielke, *J. Phys. A* **24**, L73 (1991); M. Ulmke, *Eur. Phys. J. B* **1**, 301 (1998); T. Okabe, cond-mat/9707032; L. Bartosch, M. Kollar, and P. Kopietz, *Phys. Rev. B* **67**, 092403 (2003); A. Mielke, *Phys. Lett. A* **174**, 443 (1993); H. Tasaki, *Phys. Rev. Lett.* **75**, 4678 (1995); S. Daul and R. M. Noack, *Phys. Rev. B* **58**, 2635 (1998), and reference therein.
- <sup>14</sup> J. Solyom, *Adv. Phys.* **28**, 201 (1979); J. Voit, *Rep. Prog. Phys.* **58**, 977 (1995); T. Giamarchi, *Quantum Physics in One Dimension*, (Oxford University Press, USA, 2004).
- <sup>15</sup> R. Klesse and A. Stern, *Phys. Rev. B* **62**, 16912 (2000); V. V. Ponomarenko and D. V. Averin, *Phys. Rev. Lett.* **85**, 4928 (2000).
- <sup>16</sup> E. Lieb and D. Mattis, *Phys. Rev.* **125**, 164 (1962).
- <sup>17</sup> N. D. Mermin and H. Wagner, *Phys. Rev. Lett.* **17**, 1133 (1966).
- <sup>18</sup> L. Mathey, E. Altman, and A. Vishwanath, *Phys. Rev. Lett.* **100**, 240401 (2008).